Co-expression of dimethyl sulfide monooxygenase by single vector dual promoter strategy

by

Zacheriah Minton Alexander

Honors Thesis

Appalachian State University

Submitted to the Department of Chemistry
and The Honors College
in partial fulfillment of the requirements for the degree of

Bachelor of Science

December, 2018

Approved by:

Megen Culpepper, Ph.D., Thesis Director

Brooke Christian, Ph.D., Second Reader

Ted Zerucha, Ph.D., Second Reader

Libby Puckett, Ph.D., Departmental Honors Director

Jefford Vahlbusch, Ph.D., Dean, The Honors College

Acknowledgements

This research was made possible by the Appalachian State University's A.R. Smith Department of Chemistry along with funding supplied by the National Institutes of Health (NIH). Also, previous advances made by members of the Culpepper lab aided in the development of this co-expression study. I have also been provided generous scholarships from the Smith and Whitaker families that have provided me with additional means during my academic career. I would like to express my very great appreciation to those that have made it possible for me to conduct this research.

I would also like to offer my special thanks to Dr. Megen Culpepper, who generously accepted me into her lab, and guided me throughout my research. She has been a tremendous help in teaching me numerous techniques, keeping research on schedule, and offering encouragement even through failure. Her assistance in my thesis has been immeasurable.

I would like to express deep gratitude to Dr. Ted Zerucha and Dr. Brooke Christian for volunteering to be my honor's thesis committee, reading my thesis, and helping with revisions.

Abstract

Volatile organic sulfur compounds (VOSCs) are sulfur compounds that readily aerosolize in the Earth's atmosphere. These compounds play an essential role in cloud formation, global warming, and acid rain production. Of the group of VOSCs, dimethyl sulfide (DMS) is a large component with upwards of 40 million metric tons being naturally produced and released into the atmosphere resulting in nearly 75% of the total sulfur flux. Not much is known regarding the structure and function of enzymes that further breakdown DMS, but recent research has isolated an enzyme from a garden soil microbe, *Hyphomicrobium sulfonivorans*, capable of degrading DMS into methanethiol and formaldehyde termed DMS monooxygenase. DMS monooxygenase consists of two subunits: DmoA and DmoB. DmoA is a 53 kDa $FMNH_2$-dependent monooxygenase and DmoB is a 19 kDa NAD(P)H-dependent oxidoreductase. From previous research the gene sequence of *dmoA* is known; however, there are two sequence candidates for NAD(P)H-dependent oxidoreductases, *dmoB136* and *dmoB176*, encoded on the *dmo* operon. Also, from previous research protein purification from *H. sulfonivorans* suggest a strong interaction between the DmoA and DmoB subunits, providing precedence for co-expression studies. The *dmoA* gene and one of the aforementioned *dmoB* gene candidates, *dmoB136,* were cloned into a p-DUET plasmid with streptomycin resistance and a CDF replicon. The *dmoB136* gene is located in multiple cloning site 1 containing a N-terminal a His_6-tag, and the *dmoA* gene is located in multiple cloning site 2 followed by a C-terminal S-tag. The plasmid containing genes for both subunits was transformed in C41(DE3) *E. coli* and expressed. Purification strategies include affinity and size-exclusion chromatography. Initial data suggests co-expression of DmoA and DmoB with proteins at M_r 55 kDa and 16 kDa as analyzed by SDS-PAGE. The presence of DmoB is further

evidenced by initial activity assays, with higher activity in assays containing FMN as compared to those without FMN. Current research is being performed to optimize the purification strategies for isolating each subunit in order to test each for enzyme activity, kinetics, and cofactor requirements.

Table of Contents

Table of Figures

Table of Tables

Chapter I: Relevance

Introduction

The sulfur cycle maps the exchange of volatile organic sulfur compounds (VOSCS) between aquatic and terrestrial environments with the atmosphere, as shown in Figure 1. The predominant VOSC in this exchange is the molecule dimethyl sulfide (DMS).[1] VOSCs play an essential role in cloud formation, global warming, and acid rain production.[2] Acid rain is produced through the process of photochemical oxidation, which occurs when aerosolized sulfur particles are emitted into the atmosphere and react with free radicals produced from ionizing ultraviolet radiation, converting VOSCs into sulfur oxyacids (Table I). These sulfur oxyacids condense and precipitate back to earth in the form of acid rain.[2] Despite this negative consequence, an increase in atmospheric sulfur aerosols also directly increases cloud droplet nucleation sites, increasing cloud albedo.[3] Albedo affects reflectivity, allowing less radiation from the sun to be transmitted, resulting in a negative feedback cycle. The increase in sulfur aerosols is a direct result of increased DMS production by phytoplankton in warming oceans. This is the premise of the CLAW hypothesis, which is an explanation for the homeostatic relationship between VOSC formation and climate change.[4] It states that VOSC production increases with increasing global temperatures, resulting in greater cloud albedo, greater backscatter of radiation and an overall cooling effect. Under cooler global temperatures, VOSC production decreases, decreasing cloud albedo, increasing radiation and resulting in an overall global warming.[4]

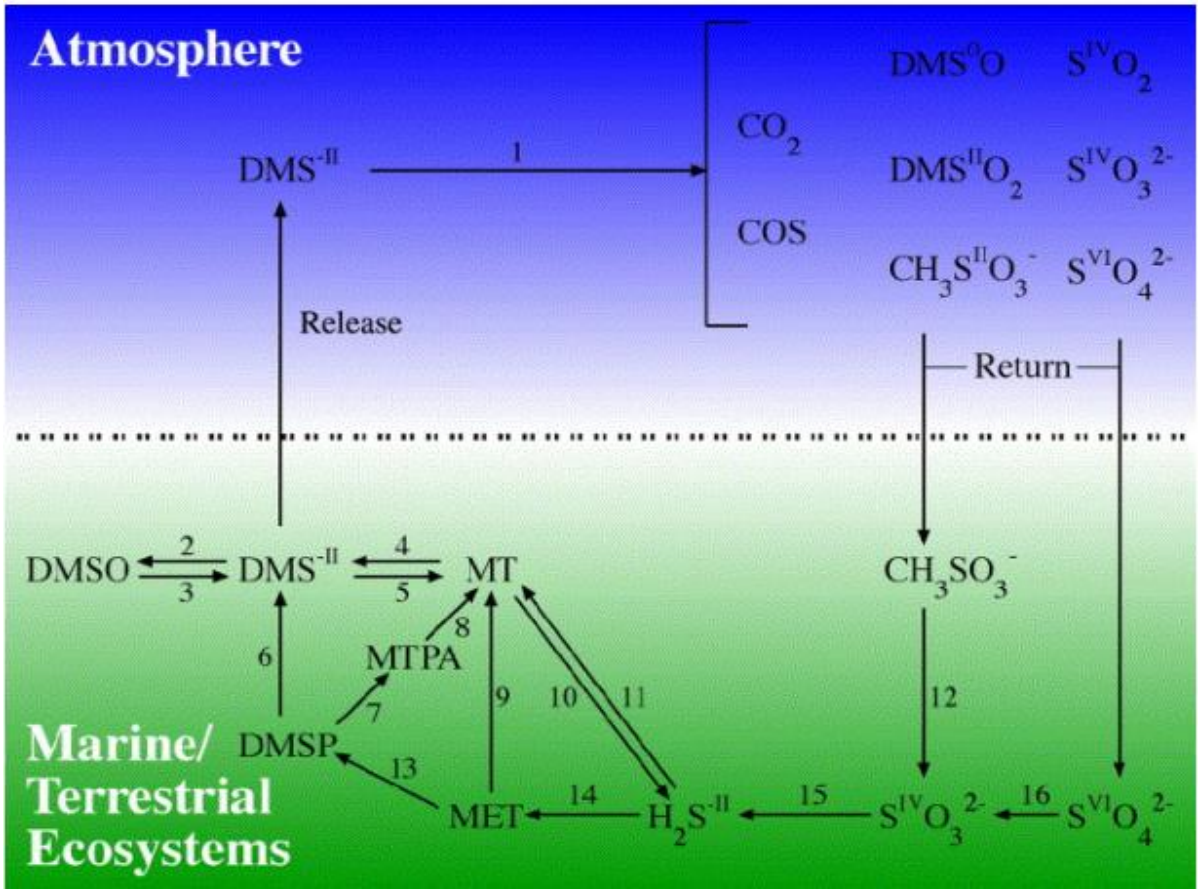

Figure 1. Sulfur cycle of VOSCs exchanged between marine and terrestrial ecosystems and the atmosphere.[2] Reaction 1 demonstrates the photochemical oxidation of VOSCs producing a variety of sulfuric oxyacids. The subsequent reactions outline the enzymatic breakdown and formation of dimethyl sulfide (DMS) prior to photochemical oxidation into the atmosphere. Reprinted from Chemosphere with permission from Elsevier.

Table I. Atmospheric sulfur oxyacids produced by photochemical oxidation.[2]

Sulfur Oxyacids			
Inorganic		**Organic**	
Sulfuric acid	H_2SO_4	Methanesulfenic acid	$CH_3–S–OH$
Sulfurous acid	H_2SO_3	Methanesulfinic acid	$CH_3–SO_2H$
Bisulfate	HSO_4^-	Methanesulfonic acid	$CH_3–SO_3H$
Bisulfite	HSO_3^-		

As stated previously, dimethyl sulfide (DMS) is the largest VOSC contributor, produced both anthropogenically and biogenically. Anthropogenically, DMS is produced through Kraft pulping, a process used to remove the lignin from wood,[5] and it is a byproduct of Swern oxidation, in which aldehydes and ketones are generated from secondary alcohols with dimethyl sulfoxide (DMSO) as the reaction solvent.[6] DMS is also produced naturally from microbial reduction of DMSO found in industrial sewage waste;[7] however, these methods produce drastically less DMS compared to phytoplankton, which produce upwards of 40 million metric tons per year and release it into the atmosphere, resulting in nearly 75% of the total sulfur flux.[8] The predominant source of DMS results from microbial metabolism. Therefore emphasis in the field should be placed on understanding the enzymatic breakdown and production of DMS from biogenic sources. The production of DMS by phytoplankton is attributed to the activity of a lyase enzyme responsible for the degradation of dimethylsulfoniopropionate (DMSP) (Figure 1, reaction 6).[2] DMSP regulates osmosis in phytoplankton and its metabolic pathway has been characterized in detail.[2] In phytoplankton, DMSP is converted to DMS and acrylate through an alkaline elimination reaction catalyzed by the enzyme DMSP lyase with high specificity.[2]

Though the formation of DMS by DMSP lyase has been characterized, less is known regarding the structure and function of enzymes in the metabolic pathway that break down DMS. Bacteria from the genus *Thiobacillus* are known to grow autotrophically using many sulfur containing compounds. Smith and Kelly isolated five strains of bacteria that grew on a number of sulfur sources such as sulfide, thiosulfate, and tetrathionate, but most importantly, the bacteria were capable of autotrophic growth using DMS.[9] This isolate also degraded DMS to CO_2 and sulfate.[9] Schafer identified strains of bacteria from the genus

Methylophaga isolated from samples of coastal seawaters that were capable of growing solely on DMS.[10] These studies also demonstrate DMS degradation.[10] No enzymes were isolated and purified in either study. The first isolation of an enzyme capable of degrading DMS has been reported and termed DMS monooxygenase.[11] The focus of this work will be placed on the characterization of DMS degradation by DMS monooxygenase from *Hyphomicrobium sulfonivorans*.

H. sulfonivorans is a garden soil microbe that metabolizes dimethylsulfone ($DMSO_2$), DMSO, and DMS (Figure 2).[11] *H. sulfonivorans* converts $DMSO_2$ to DMSO through a reaction catalyzed by $DMSO_2$ reductase, and DMSO is further reduced to DMS by a DMSO reductase.[11] DMS is then oxidized by DMS monooxygenase into methanethiol and formaldehyde.[11] The methanethiol produced is further oxidized into formaldehyde and hydrogen sulfide by methanethiol oxidase. The formaldehyde from this metabolic pathway is either oxidized to carbon dioxide or converted into biomass through the methylotrophic serine cycle.[11] Research by Boden et al. isolated and characterized the first DMS monooxygenase enzyme from *H. sulfonivorans*. The isolated enzyme consists of two subunits: DMS monooxygenase subunit A (DmoA) and DMS monooxygenase subunit B (DmoB).[11] DmoA is a 53 kDa $FMNH_2$-dependent monooxygenase and DmoB is a 19 kDa NAD(P)H-dependent oxidoreductase which reduces the FMN cofactor required by the A subunit.[11] The gene sequence of *dmoA* is known; however, there are two sequence candidates for NADH-dependent oxidoreductase that are encoded on the *dmo* operon: *orf136* and *orf176* (Figure 3).[11]

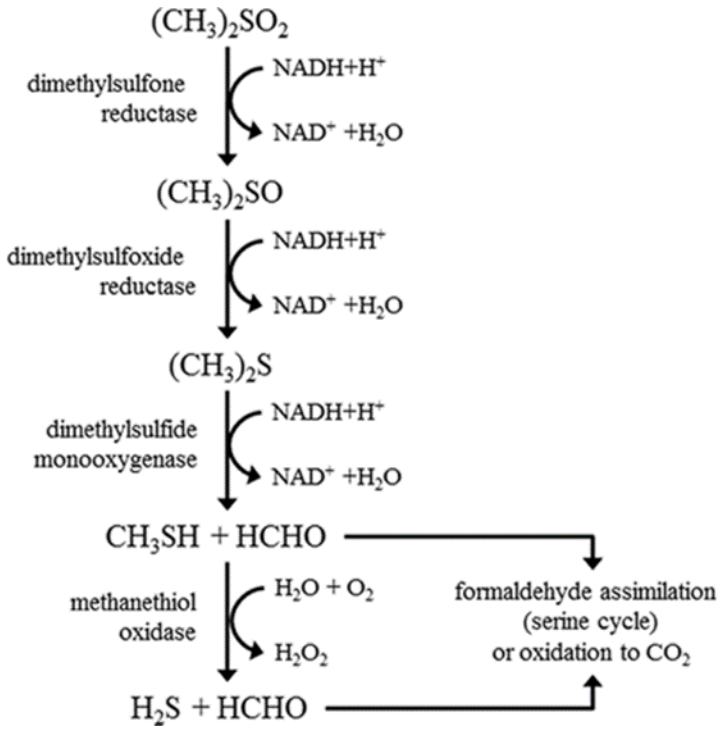

Figure 2. Metabolic pathway of DMS degradation in *Hyphomicrobium sulfonivorans*.[11] Reproduced with permission from American Society for Microbiology.

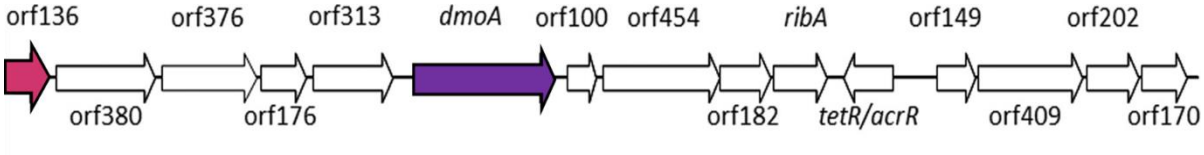

Figure 3. Native operon in *H. sulfonivorans* encoding the two-subunit protein DMS monooxygenase.[11] One gene candidate for *dmoB* is highlighted in pink, *dmoB136*, and the gene for *dmoA* is highlighted in purple. Amended with permission from American Society for Microbiology.

DMS monooxygenase belongs to the flavin-dependent two-component monooxygenase family of enzymes in which a reductase subunit reduces the flavin cofactor. The reduced flavins are supplied to the flavin-dependent monooxygenase subunit to oxidize substrates and form products.[12] In order to catalyze the conversion of reactants to products, the

monooxygenase subunit activates molecular oxygen forming a C4a-(hydro)peroxyflavin oxygenated intermediate, which can serve as either a nucleophile or an electrophile depending on the nature of the reaction.[12] One atom of the molecular oxygen is incorporated into product formation and the other atom of oxygen is reduced to water.[13] Typically, a flavin serves as a prosthetic group, but in this family of flavin-dependent monooxygenases, the flavin is used as a substrate.[12] This family of enzymes is highly diverse, so each flavin dependent monooxygenase can be classified (A-H) based on protein structure, sequence motifs, electron donors, and reaction type.[13] It is proposed that the DmoB subunit reduces FMN to $FMNH_2$ by oxidizing NADH.[11] The $FMNH_2$ is then supplied to the DmoA subunit, allowing DmoA to oxidize DMS into methanethiol and formaldehyde, as shown in Figure 4. Based on this proposition, DMS monooxygenase is believed to be a class C monooxygenase as it is a two-component monooxygenase with an NAD(P)H-dependent oxidoreductase that reduces FMN.[13] Also, the monooxygenase subunit requires $FMNH_2$ as an electron donor which is exemplary of a class C flavin-dependent monooxygenase.[13]

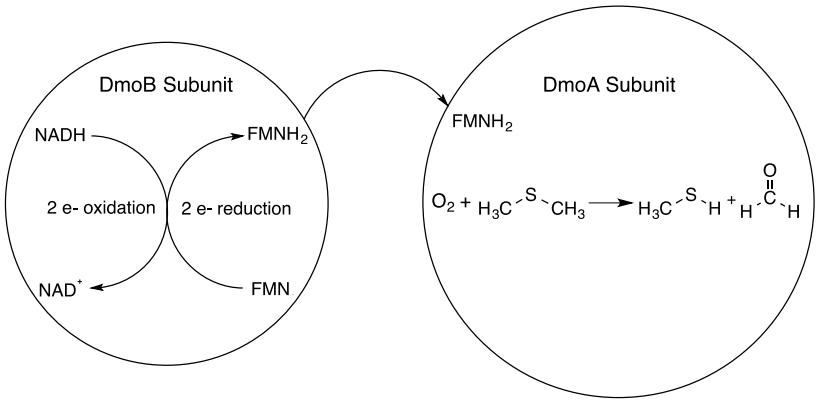

Figure 4. Chemical reaction and subunit interaction of DMS monooxygenase

The work by Boden and coworkers isolated the native DMS monooxygenase from *H. sulfonivorans* and minimal characterization was performed.[11] The SDS-PAGE gel analyzed by Boden and coworkers indicates that the DmoA and DmoB subunits tightly associate in the native protein due to stoichiometric amounts of each protein after multiple rounds of purification.[11] Previous studies in the Culpepper lab have attempted to express each subunit individually and recombinantly in *E. coli* toward characterizing the enzyme; however, individual expression of the DmoB subunit leads to the formation of inclusion bodies. Based on the interaction observed in the natively isolated protein and trouble expressing the DmoB subunit in *E. coli*, co-expression studies using a single vector dual promoter strategy were initiated. Studies also include co-expression optimization and purification strategies to isolate both subunits recombinantly in order to study the enzyme activity and kinetics. The focus of this project is to engineer a single vector (pCDFDUET-1) containing the genes of both *dmoB* and *dmoA,* optimize growth for protein co-expression, and analyze enzyme kinetics and activity in DMS degradation. The hypothesis of this study is that expression of both subunits simultaneously will allow for the successful expression of DmoB136, and that through co-expression, a tight association between DmoB136 and DmoA will be observed similar to the native protein.

Chapter II: Molecular Cloning of Recombinant Plasmid

Introduction

Co-expression of two proteins simultaneously can be performed using either multiple vectors or a single vector. In a multiple vector strategy, each plasmid must contain a gene for a subunit and a gene for antibiotic resistance.[14] Also the replicon on each vector needs to be compatible for optimal co-expression.[14] A single vector approach requires a plasmid with more than one multiple cloning site, with different restriction enzyme cut sites.[14] Each gene can be controlled by multiple promoters or a single promoter, resulting in multiple RNAs or a long polycistronic RNA, respectively.[14] Studies have shown that expression with polycistronic RNA results in a decrease in expression of genes further downstream on the RNA,[14] so to avoid the complexities of a multiple vector approach and avoid the risk of losing protein expression due to polycistronic RNA, a single vector dual promoter strategy was adopted to co-express DmoB and DmoA.

Previous work on two-component flavin dependent monooxygenases have shown the co-expression proof of principle to work utilizing each of the previous strategies. Lee and Zhao studied a two-component arylamine oxygenase with PrnD being the *N*-oxygenase and PrnF suspected to be the flavin reductase.[15] Using a multiple vector approach a pACYC-Duet vector containing the *prnF* gene and a pTKXb119 vector containing the *prnD* gene were engineered, co-expressed in BL21(DE3), purified using affinity chromatography, and successfully characterized using various spectroscopic techniques.[15] The multiple vector approach was employed in this study as Lee and Zhao had already previously engineered their pTKXb-PrnD vector. Research by Chen et al. analyzed the metabolism of UWM6 to produce

jadomycin A by oxygenases JadF and JadG and oxygenase/dehydrogenase JadH.[16] A pUWL201 vector containing the *jadF, jadG,* and *jadH* genes was engineered and transformed in *Streptomyces lividans*.[16] Bioconversion assays, *in vivo* and *in vitro*, were used to analyze activity of co-expressing cells.[16] A polycistronic single vector approach was implemented, since each of the studied genes occurred in sequence in the jadomycin biosynthetic operon. Furthermore, research by Blake et al. studied human cytochrome P450 monooxygenase systems recombinantly expressed in *E. coli*. [17] Previous research has shown low activity in recombinantly expressing cells, as there isn't a native P450 reductase in *E. coli* that is highly compatible with the P450 monooxygenase.[17] As a result, Blake et al. engineered a dual promoter vector containing the gene for cytochrome P450 3A4 (CYP3A4), a monooxygenase, and the gene for a P450 reductase, each controlled by their own *lac* promoter.[17] From their results, no activity was seen when proteins were expressed individually, but transformants containing co-expressed protein saw high specific activities that were better than other recombinant systems previously reported.[17]

The focus of this project is to engineer a vector (pCDFDUET-1) containing the genes of both *dmoB* and *dmoA,* optimize growth for protein co-expression, and analyze enzyme kinetics and activity in DMS degradation. The *dmoA* gene and the *dmoB* gene candidate, *dmoB136*, were cloned into a plasmid containing dual promoters and ribosomal binding sites. The *dmoB136* gene was cloned into multiple cloning site 1 (MCS1) containing an N-terminal His_6-tag, and the *dmoA* gene was cloned in MCS2 containing a C-terminal S-tag, resembling the gene arrangement on the native operon. The step-wise process for engineering the recombinant plasmid, *dmoB136-dmoA*-pCDFDuet-1, is shown in Figure 5.

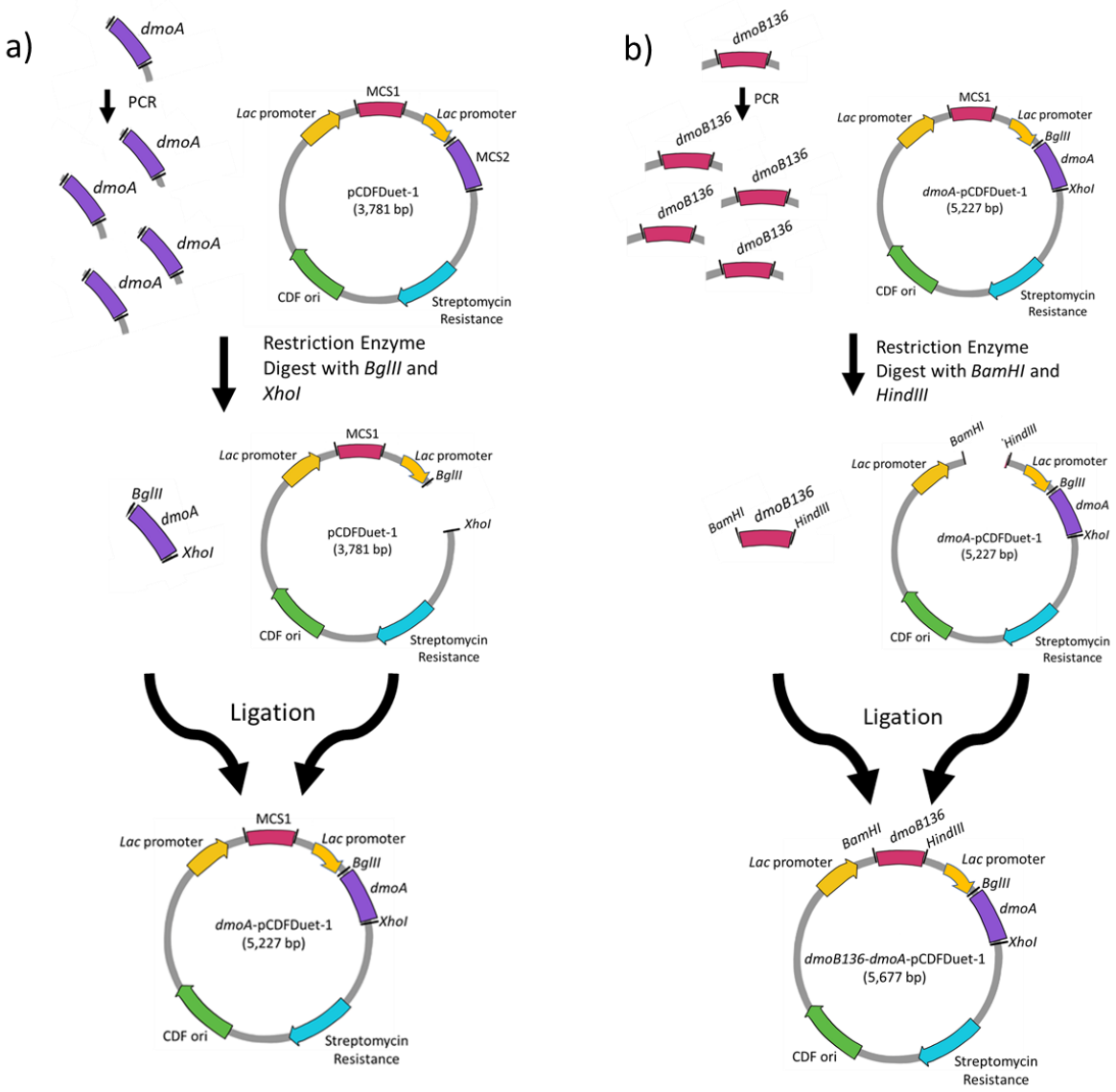

Figure 5. Strategy for subsequent cloning of *dmoA*-pCDFDuet-1 (a) and *dmoB136-dmoA*-pCDFDuet-1 (b).

Materials and Methods

Polymerase chain reaction of dmoA and dmoB136

The *dmoA* gene template, originally cloned into a pET-21a vector, was amplified by adding ~100 ng of *dmoA*-pET-21a, 2 µM Reverse primer (dmoA_B_R_Stag, Table II), 2 µM Forward primer (A_site2_bglII_F, Table II), PCR master mix (0.025 U/µL Taq DNA polymerase,

reaction buffer, 2 mM $MgCl_2$, 0.2 mM of each dNTP (dATP, dCTP, dGTP and dTTP); ThermoFisher), and sterile water. The polymerase chain reaction (PCR) was performed using a PTC-200 Thermal Cycler (MJ Research) with the parameters listed in Table III.

The *dmoB136* gene template, originally cloned into a pet-21a vector, was amplified by adding ~100 ng of *dmoB136*-pET-21a, 2 µM of Reverse primer (B136-1-Stag-R-New, Table II), 2 µM of Forward primer (B136_1-BamHI_F, Table II), PCR master mix (0.025 U/µL Taq DNA polymerase, reaction buffer, 2 mM $MgCl_2$, 0.2 mM of each dNTP (dATP, dCTP, dGTP and dTTP); ThermoFisher), and sterile water. PCR was performed using a PTC-200 Thermal Cycler (MJ Research) with the parameters listed in Table III. The PCR products for *dmoA* and *dmoB136* were purified using a Qiagen QIAquick PCR Purification Kit.

Table II. Names and sequences of DNA primers

DNA Primers	
Name	**Sequence**
A_site2_BglII_F	5’-GATCAGATCTATGAAAAAACGTATCG-3’
dmoA_B_R_Stag	5’-ATTTCTCGAGTTCGGCCACC-3’
B136_1-BamHI_F	5’-GATCGGATCCATGAGCTGTACC-3’
B136-1-Stag-R-New	5’-GATCAAGCTTGCTGGCCAGTG-3’
DuetUP1	5’- GGATCTCGACGCTCTCCCT-3’
DuetDOWN1	5’- GATTATGCGGCCGTGTACAA-3’
DuetUP2	5’- TTGTACACGGCCGCATAATC-3’
T7term	5’- CTAGTTATTGCTCAGCGG-3’

Table III. Parameters of PCR for amplification of *dmoA* and *dmoB136*

dmoA			***dmoB136***		
Temperature (°C)	**Time (s)**	**Cycles**	**Temperature (°C)**	**Time (s)**	**Cycles**
95	90	1	95	180	1
95	30	35	95	60	30
58	30	35	50	60	30
72	90	35	72	60	30
72	300	1	72	300	1

DNA gel electrophoresis of PCR products

The *dmoA* and *dmoB136* PCR products were analyzed by agarose gel electrophoresis. A 1% agarose gel was prepared in TAE buffer (40 mM Tris, 20 mM acetic acid, 1 mM EDTA) and heated until the agarose dissolved. To the solution, RedSafe™ Nucleic Acid Staining Solution (iNtRON) was added, and the gel was cooled to solidify. DNA loading dye (LD; 1.7 mM Tris-HCl (pH 7.6) 0.005% bromophenol blue, 0.005% xylene cyanol FF, 10% glycerol, 10 mM EDTA; ThermoFisher) was added to each PCR product. Gels were run at 100 V for 1 hour and the DNA sizes were compared with a 1 Kb GeneRuler DNA Ladder (0.5 µg/µL; ThermoFisher).

Restriction enzyme double digest on purified PCR products

A restriction enzyme double digest was performed on the purified *dmoA* PCR product and the pCDFDuet-1 plasmid using *BglII* and *XhoI*, followed by another digest on *dmoB136* and the recombinant plasmid *dmoA*-pCDFDuet-1 using *BamHI* and *HindIII* (Figure 5). The double digest of *dmoA* and pCDFDuet-1 was set up by adding ~1500 ng of pCDFDuet-1 or purified *dmoA* PCR product to separate tubes. The pCDFDuet-1 vector and purified *dmoA* PCR

product were digested with 333 U/mL *BglII* (NEB) and 667 U/mL *XhoI* (NEB), in NEBuffer 3.1 (100 mM NaCl, 50 mM Tris-HCl (pH 7.9), 10 mM $MgCl_2$, 100 µg/ml BSA; NEB) and sterile water. The linearized plasmid was prevented from re-ligating by treating it with 333 U/mL CIP to dephosphorylate the 5' end of the linear DNA.

The double digest of *dmoB136* and *dmoA*-pCDFDuet-1 was set up by adding ~1500 ng of *dmoA*-pCDFDuet-1 or purified *dmoB136* PCR product to separate tubes. The *dmoA*-pCDFDuet-1 vector and the purified *dmoB136* PCR product were digested with 333 U/mL of *BamHI* and 333 U/mL *HindIII*, in CutSmart buffer (50 mM potassium acetate, 20 mM Tris-acetate, 10 mM magnesium acetate, 100 µg/ml BSA, pH 7.9) and sterile water. The linearized plasmid was prevented from re-ligating by treating it with 333 U/mL CIP to dephosphorylate the 5' end of the linear DNA. All tubes were digested at 37 °C for 1 hour. The digested DNA was purified using a Qiagen QIAquick PCR Purification Kit and the concentrations were determined using a NanoDrop 2000c Spectrophotometer (ThermoFisher).

Ligation of digested plasmids and inserts

The ligation of *dmoA* and pCDFDuet-1 was set up by adding ~100 ng of digested *dmoA*, ~25 ng of digested pCDFDuet-1, 0.5 U/µL of T4 Ligase (Invitrogen), and ligase buffer (50 mM Tris-HCl (pH 7.6), 10 mM $MgCl_2$, 1 mM ATP, 1 mM DTT, 5% (w/v) polyethylene glycol-8000; Invitrogen). A negative control ligation was set up by adding the same components and concentrations for the experimental ligation but the *dmoA* insert was replaced with sterile water.

Ligations of *dmoB136* and *dmoA*-pCDFDuet-1 were set up with two different vector to insert ratios (1:1 and 1:7 by weight). The 1:1 ligation was performed by adding 35 ng of

digested *dmoB136*, 35 ng of digested *dmoA*-pCDFDuet-1, 40 U/ µL T4 Ligase (NEB), ligase buffer (50 mM Tris-HCl (pH 7.5), 10 mM $MgCl_2$, 1 mM ATP, 10 mM DTT; NEB), and sterile water. The 1:7 ligation was performed by adding 250 ng of digested *dmoB136*, 35 ng of digested *dmoA*-pCDFDuet-1, 40 U/µL of T4 Ligase (NEB), and ligase buffer (50 mM Tris-HCl (pH 7.5), 10 mM $MgCl_2$, 1 mM ATP, 10 mM DTT; NEB). A negative control ligation was set up by adding the same components and concentrations for the 1:7 experimental ligation but the *dmoB136* insert was replaced with sterile water. Each tube was mixed thoroughly, and each ligation was aliquoted into separate tubes. One of each of the aliquots for the ligation of *dmoA* and pCDFDuet-1 were ligated at 16 °C for 16 hours and then the temperature was decreased to 4 °C, and the other aliquots were ligated at 4 °C overnight. One of each of the aliquots for the ligation of *dmoB136* and *dmoA*-pCDFDuet-1 were ligated at 16 °C overnight, and the other aliquots were ligated at room temperature overnight. Following these steps, each ligation of *dmoB136* and *dmoA*-pCDFDuet-1 was incubated at 65 °C for 10 minutes to inactivate the ligase.

Ligation reactions were transformed into DH5α- competent *E. coli* cells (Invitrogen), plated on a LB agar plate containing 50 µg/mL streptomycin, and incubated overnight at 37 °C. Individual colonies were grown in sterile-LB media containing 50 µg/mL streptomycin shaking at 220 rpm, at 37 °C, overnight. The cell pellet was then isolated, resuspended and the plasmid extracted using a Qiagen QIAprep Spin Miniprep Kit.

Screening ligation reactions by double digestion

A restriction enzyme double digest using *BamHI* and *XhoI* was performed on nine ligated plasmids (*dmoB136*-*dmoA*-pCDFD-1). For the experimental digestions, each ligated

plasmid was digested with 333 U/mL of *BamHI* and 667 U/mL of *XhoI*, in CutSmart (50 mM potassium acetate, 20 mM Tris-acetate, 10 mM magnesium acetate, 100 µg/mL BSA, pH 7.9; NEB) and sterile water. All tubes were digested at 37 °C for 1 hour. The restriction enzyme double digests were analyzed using gel electrophoresis as previously described. The ligated plasmid was sequenced by Sanger sequencing (Eurofins genomics) for verification using DuetUP1 and DuetDOWN1 sequencing primers for MCS1 and DuetUP2 and T7term sequencing primers for MCS2 (Table II).

Results

The genes for *dmoA* and *dmoB136* from *H. sulfonivorans* were successfully amplified by PCR (Figure 6a and b). Figure 6a lane 2 shows amplification of a single species at ~ 1500 bp when compared with the GeneRuler 1 kb DNA Ladder. Figure 6b lane 2 also indicates amplification of a single gene at ~ 500 bp compared with the GeneRuler 1 kb DNA Ladder.

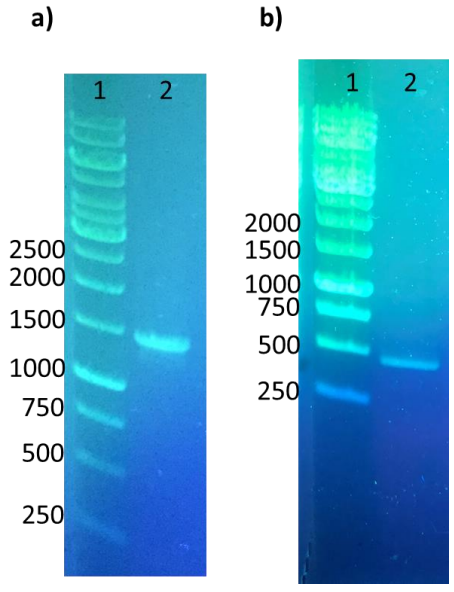

Figure 6. Amplification of *dmoA* (a) and *dmoB136* (b) genes via PCR. The PCR reactions were analyzed by agarose gel electrophoresis. Gels were made containing RedSafe™ Nucleic Acid Staining Solution to visualize DNA bands. Lane 1 in (a) and (b) corresponds to the GeneRuler. Lane 2 in (a) and (b) corresponds to each PCR product.

The amplified products were digested and sequentially ligated into the pCDFDuet-1 vector using the approach illustrated in Figure 5. The vector *dmoB136-dmoA*-pCDFDuet-1 was digested with *BamHI* and *XhoI* to analyze for the successful insertion of both *dmoB136* and *dmoA* genes. In Figure 7, lane 2 the single band indicates an unsuccessful digestion with a at ~ 5500 bp. This nucleotide size corresponds to an uncut plasmid containing both genes. Lanes 3, 4, 5, 6, 8, and 10 contain two bands at ~ 3500 bp and ~ 2000 bp. These results indicate a successful digestion and successful insertion of both genes into the vector. Lastly, lanes 7 and 9 also contain two bands corresponding to genes at ~ 3500 bp and another at ~ 1500bp. These results demonstrate a successful digest, but insertion of only *dmoA* into the vector (Figure 7).

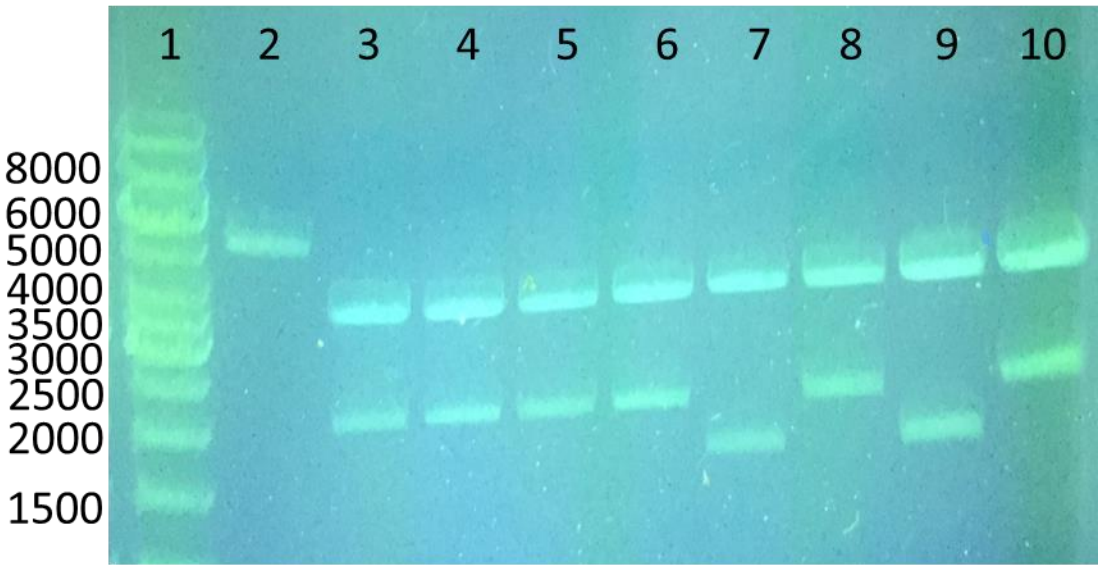

Figure 7. Digestion of *dmoB136-dmoA*-pCDFDuet-1 with *BamHI* and *XhoI*. Lane 1 indicates the GeneRuler DNA ladder. Lanes 2-10 indicate individual ligation reactions screened by double digestion with *BamHI* and *XhoI*.

The ligated plasmid containing *dmoA*-pCDFDuet-1 (plasmid from Lanes 7 and 9 in Figure 7) was sequenced and aligned to the known sequence of *dmoA*. The sequence alignment resulted in an overlap of 1,224 bp out of the total 1,446 bp in the *dmoA* sequence.

The middle 222 bp of the vector and three mismatches were likely not sequenced as a result of the T7 DNA polymerase efficiency. An internal primer is necessary to read this portion of the gene.

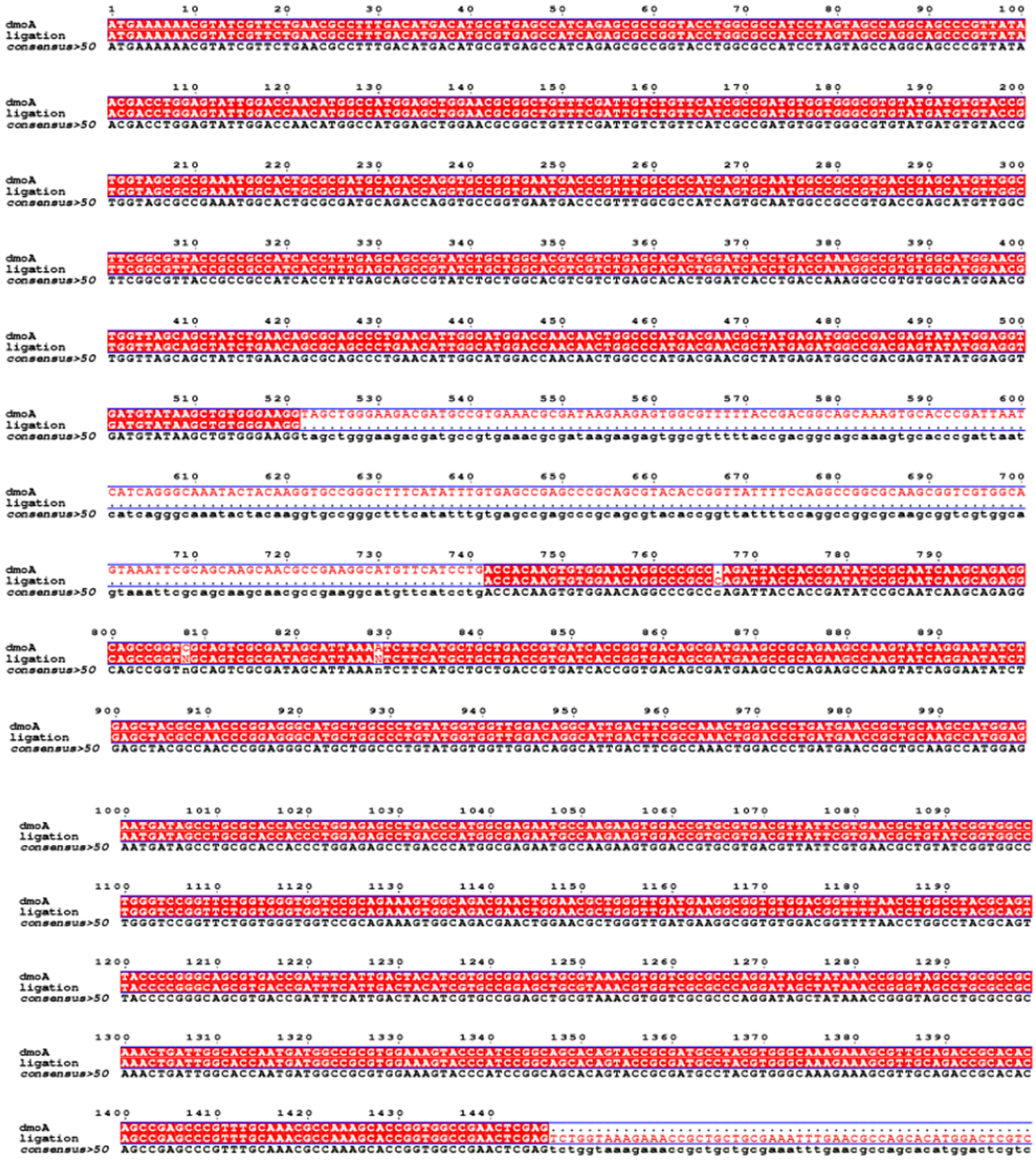

Figure 8. Sequencing of *dmoA*-pCDFDuet-1 ligation reaction aligned with the gene sequence for *dmoA* using MultAlin.[18] The top row of the gene sequence shows the known gene sequence of *dmoA*. The middle row shows the gene sequence for the ligation reaction, and the bottom row shows the consensus between the top two sequences. Areas highlighted in red indicate conservation between the gene sequences.

The ligated plasmid containing *dmoB136-dmoA*-pCDFDuet-1 was sequenced and aligned to the known sequence for *dmob136* from *H. sulfonivorans*. The sequence overlapped at 450 out of the 450 base pairs, yielding a 100% identical sequence.

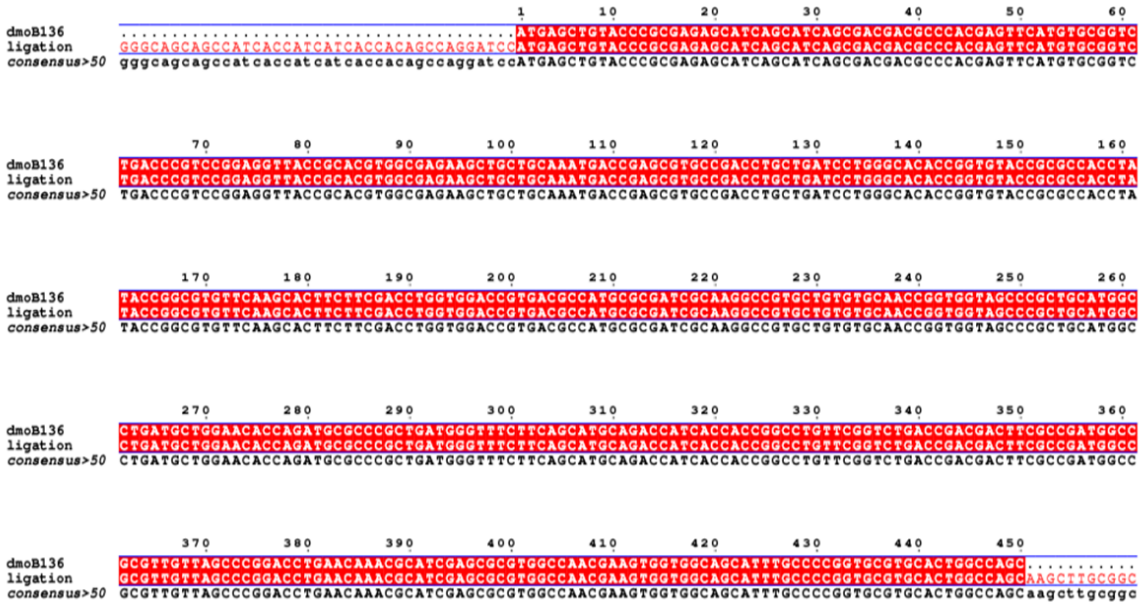

Figure 9. Sequencing of *dmoB136-dmoA*-pCDFDuet-1 aligned with the gene sequence for *dmoB136* using MultAlin.[18] The top row of the gene sequence shows the known gene sequence of *dmob136*. The middle row shows the gene sequence for the recombinant plasmid, and the bottom row shows the consensus between the top two sequences. Areas highlighted in red indicate alignment between the gene sequences.

Discussion

From the gels containing the *dmoA* or *dmoB136* PCR amplification, the size of the purified PCR products can be determined by comparison with the GeneRuler 1 kb DNA Ladder. The PCR product for *dmoA* is approximately 1500 bp (Figure 6a) which is consistent with its predicted size of 1446 bp. The PCR product for *dmoB136* is approximately 500 bp (Figure 6b) which is consistent with its predicted size of 450 bp. These results indicate that

the primers were specific for the genes of interest and the annealing temperatures and extension times were optimal for gene amplification.

Once the PCR products were obtained, restriction enzyme digestion followed by sequential ligation reactions were performed. The end goal is to insert the *dmoA* gene into Multiple Cloning Site 2 (MCS2) in the pCDFDuet-1 vector, followed by subsequent digest and ligation of the *dmoB136* into MCS1 of pCDFDuet-1 to obtain the complete vector required to initiate coexpression studies of DMS monooxygenase. From the gel containing *dmoB136*-*dmoA*-pCDFDuet1 digested with *BamHI* and *XhoI*, the size of each resulting fragment can be compared with the GeneRuler 1 kb DNA Ladder (Figure 7). Lane 2 contained a fragment size around 5,500 bp, which indicates that though the plasmid digestion was unsuccessful, the genes (1,446bp and 450 bp) were ligated into the empty pCDFDuet-1 vector (3,781 bp). In Figure 7, lanes 7 and 9 both contained fragment sizes around 3,500 bp, and 1,500 bp. These bands correspond to the expected fragment sizes (3,533 bp and 1,694 bp) produced when *dmoA*-pCDFDuet-1 is digested with *BamHI* and *XhoI*. This result confirms that a gene the same size as *dmoA* was inserted into pCDFDuet-1 at MCS-2. Lanes 3, 4, 5, 6, 8, and 10 in Figure 7 each contained fragment sizes around 3,500 bp, and 2,000bp. These bands correspond to the two expected fragment sizes (3,533 bp and 2,144 bp) produced when *dmoB136-dmoA*-pCDFDuet-1 is cut with *BamHI* and *XhoI*. This result confirms that a gene the same size as *dmoB136* was inserted into *dmoA*-pCDFDuet-1.

The digestion results indicate that *dmoA* was inserted into pCDFDuet-1 at MCS-2 and subsequently, *dmoB136* was inserted into *dmoA*-pCDFDuet-1 at MCS-1. To substantiate this result, the ligated plasmids were sequenced. The sequencing of the MCS2 locus of *dmoA*--

pCDFDuet-1 when aligned with the known sequence for *dmoA* resulting in an overlap of 1,224 bp out of the total 1,446 bp, meaning that *dmoA* was likely successfully inserted into MCS2. An efficiency error in the T7 DNA polymerase likely caused the middle 222 bp of the vector to not be sequenced along with three mismatches. The sequencing chromatograph was reviewed, and the mutations were determined to be silent. In addition, the plasmid containing the original *dmoA* gene in pet21b has been sequenced entirely. The sequencing of the MCS1 locus of *dmoB136*-*dmoA*-pCDFDuet-1 when aligned with the known sequence for *dmoB136* produced a 100% base pair match, meaning that *dmoB136* was successfully inserted into MCS1.

Chapter III: Expression, Purification, and Activity

Introduction

Following the successful cloning of the *dmoB136-dmoA*-pCDFDuet-1 plasmid, protein expression screening was performed according to the work flow represented in Figure 10 by varying factors such as *E. coli* cell lines, expression temperatures, and Isopropyl β-D-1-thiogalactopyranoside (IPTG) concentrations in order to determine conditions for optimal protein co-expression (Figure 11). Temperature can influence the expression of recombinant protein by controlling protein synthesis and cell growth.[19] At low temperatures, cell growth and protein synthesis rates are reduced which can prevent the formation of inclusion bodies, but at high temperatures cell growth rate is increased can potentially result in plasmid loss.[19] Although recombinant protein expression generally favors short growth and high temperature, in bacteria some protein expressions favor longer growths at lower temperatures,[19] so temperatures were screened at 37 °C and 16 °C in order to determine optimal temperature for protein expression (Figure 11). The expression of recombinant protein can also be influenced by the concentration of the inducer, IPTG. At low inducer concentrations, the recombinant plasmid may not be sufficiently induced resulting in an overall lower yield of recombinant protein, but at high inducer concentrations, IPTG can become toxic, reducing cell growth and recombinant protein yield.[19] IPTG concentrations were screened at 200 µM, 500 µM, and 1 mM in order to determine the optimal inducer concentration for protein expression (Figure 11).

The cell lines screened were BL21(DE3), C41(DE3), C43(DE3), Origami B(DE3), and Rosetta-gami B(DE3). These cell lines have unique characteristics that allow for different

types of protein expression; however, all (DE3) strains contain an IPTG inducible T7 RNA polymerase, designed for vectors containing T7 promoters.[20] The BL21(DE3) cell line is a derivative of B834 used for general protein expression containing mutations in *lon* and *ompT* proteases.[20] The C41(DE3) cell line is a BL21(DE3) derivative containing a mutation that prevents cell death in the presence of toxic proteins by reducing the levels of T7 RNAP activity, and C43(DE3) is a derivative of C41(DE3) that contains an additional mutation giving it a higher tolerance for toxic protein expression.[21] The Origami B(DE3) cell line is a Tuner™ derivative that also contains a mutation in thioredoxin reductase (*trxB*) and glutathione reductase (*gor*) genes. Being a Tuner™ derivative allows for uniform IPTG entry, enabling adjustable protein expression, and the *trxB*/*gor* mutation enhances cytoplasmic disulfide bond formation.[20] The Rosetta-gami B(DE3) strain is an Origami B(DE3) derivative maintaining all its original capabilities with the addition of enhancing eukaryotic gene expression in *E. coli* by supplying six rare tRNAs.[20] After screening, the optimal growth conditions for DmoB136 and DmoA co-expression was determined in C41(DE3) *E. coli* grown at 16 °C overnight post-induction with 500 µM IPTG.

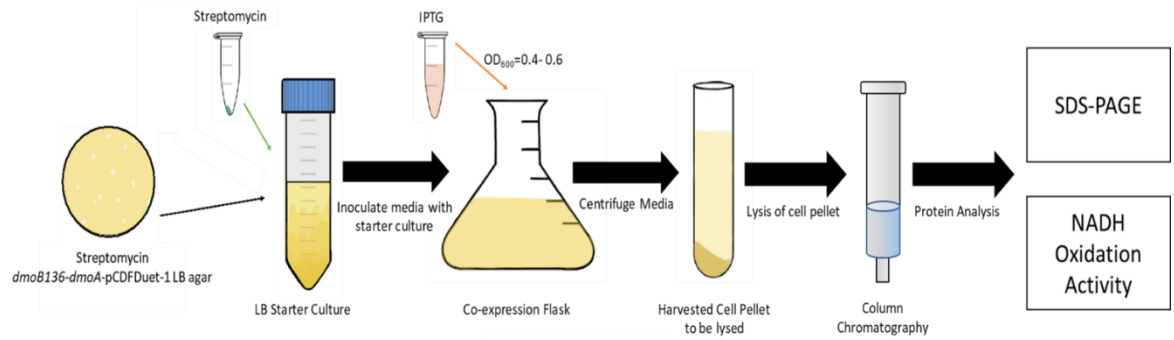

Figure 10. Strategy of growth, purification, and analysis of protein co-expression

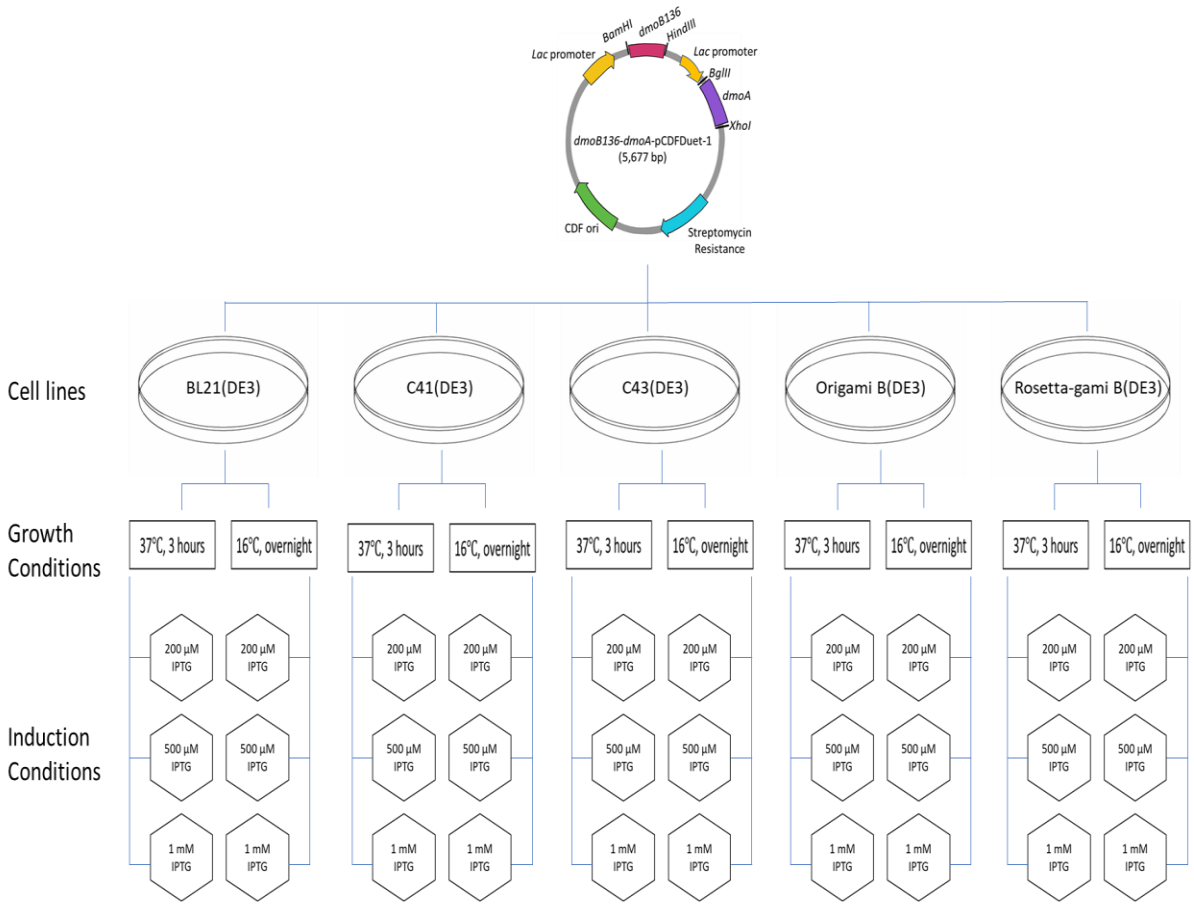

Figure 11. Protein co-expression screening in different cell lines, growth conditions, and induction conditions. A total of thirty conditions were screened in these studies.

Boden and coworkers used two consecutive rounds of size exclusion chromatography followed by one round of hydrophobic interaction chromatography to isolate both subunits in native DMS monooxygenase.[11] A Superdex200 PG was initially used, active fractions from this column were pooled, followed by a Sephadex G75 column.[11] Active fractions from the Sephadex G75 column were pooled and run on a phenyl-Sepharose column.[11] A similar purification strategy was employed to isolate the DmoA and DmoB136 expressed; however, Immobilized metal affinity chromatography (IMAC) using Nickel was incorporated due to a His_6-tag on the dmoB136 gene.

The enzyme DmoB136 is an NADH-dependent oxidoreductase. The oxidation of NADH to NAD^+ is coupled with the reduction of FMN to $FMNH_2$. NADH absorbs at 340 nm, and NAD^+ absorbs at 259 nm,[22] allowing protein activity to be measured in real time (Figure 12). The specific activity of DmoB136 can then be calculated by incorporating total milligrams of protein added to each reaction.

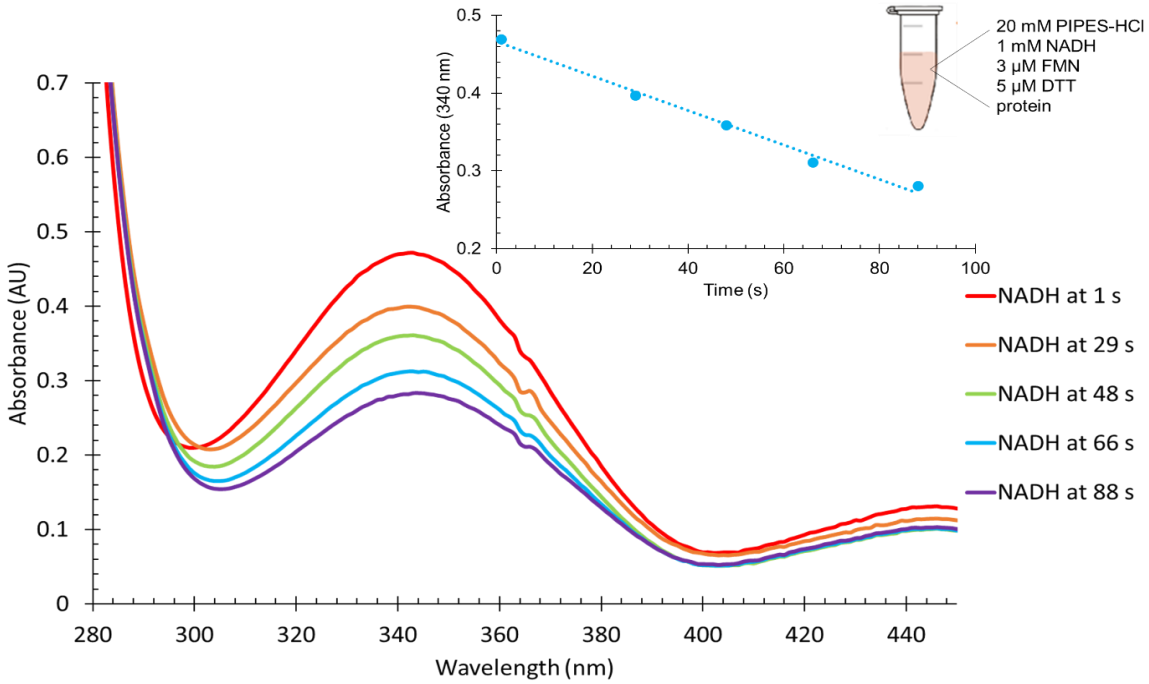

Figure 12. Reaction conditions and absorbance spectra of NADH oxidation by DmoB136. Inset graph displays the absorbance at 340nm over time.

Materials and Methods

Cell line screening

Plasmid containing *dmoB136-dmoA*-pCDFDuet-1 were transformed into all competent cell lines illustrated in Figure 11. A single colony was used to inoculate a 1 mL culture of LB-broth containing streptomycin (50 μg/mL) and incubated overnight at 37 °C at 220 rpm. The overnight culture was added to 100 mL LB-broth containing streptomycin (50

μg/mL), incubated at 37 °C at 220 rpm until the Optical Density at 600 nm was between 0.4 and 0.6. The 100 mL cultures were either induced immediately with 200 μM, 500 μM or 1mM isopropyl β-D-1-thiogalactopyranoside (IPTG) or cold shocked at 4 °C for 1 hr before induction. Immediately induced 100 mL cultures were incubated at 37 °C for 3 hours, and cold shocked cultures were incubated 16 °C overnight at 220 rpm. Cells were harvested by centrifugation at 4200 rpm, 4 °C, resuspended in buffer A (50 mM Tris, 500 mM NaCl, 10% glycerol, pH 8.0), and stored at -20 °C.

Aliquots of harvested cells were massed and 1 mM EDTA was added to the pellet. B-PER Complete Bacterial Protein Extraction Reagent (ThermoFisher) was warmed to room temperature, and 5 mL/g was added to harvested cells. The lysis mixture was incubated with gentle rocking for 30 minutes at room temperature. Soluble and insoluble proteins were separated by centrifugation at 16,000 G, 4 °C, and insoluble proteins were resuspended in buffer A (50 mM Tris, 500 mM NaCl, 10% glycerol, pH 8.0). Proteins were analyzed by SDS-PAGE as described below.

Frozen, resuspended cells were thawed, massed, mixed with 5 mL/g buffer A (50 mM Tris, 500 mM NaCl, 10% glycerol, pH 8.0) and lysozyme (1 mg/mL), and incubated at room temperature for 30 minutes with gently mixing. Cells were lysed using a Q700 sonicator (Qsonica) with a total run time of 10 minutes, 10 second pulse-on and 30 second pulse-off at an amplitude of 40.0 amplitude. Lysed cells were centrifuged at 11,000 rpm, 4 °C, for 1 hour and the supernatant was collected.

Each cell soluble lysate was manually loaded onto a HisPur Ni-NTA Spin Columns, 0.2 mL resin bed (ThermoFisher) previously equilibrated with 10 column volumes (CV) of

Buffer A (50 mM Tris pH 8.0, 500 mM NaCl, 10% glycerol). Nonspecific proteins were removed following a 10 CV wash with Buffer A. A stepwise imidazole elution of 20 mM, 100 mM, 250 mM, and 500 mM imidazole in 50 mM Tris pH 8.0, 500 mM NaCl, and 10% glycerol was performed for 5 CVs each. Fractions were collected and analyzed by SDS-PAGE as described below.

Protein expression of DmoB136 and DmoA in *C41(DE3) E. coli*

Plasmids containing *dmoB136-dmoA*-pCDFDuet-1 were transformed into C41(DE3) *E. coli* (Lucigen) cells. A single colony was used to inoculate a 10 mL culture of LB-broth containing streptomycin (50 µg/mL) incubated overnight at 37 °C at 220 rpm. The overnight culture was added to 1 L LB-broth containing streptomycin (50 µg/mL), incubated at 37 °C at 220 rpm until the Optical Density at 600 nm was between 0.4 and 0.6. The 1 L cultures were cold shocked at 4 °C for 1 hr before induction. After at least 1 hour, each 1 L culture was induced with 500 µM IPTG followed by incubation at 16 °C overnight at 220 rpm. Cells were harvested by centrifugation at 4200 rpm, 4 °C, resuspended in buffer A (50 mM Tris, 500 mM NaCl, 10% glycerol, pH 8.0), and stored at -20 °C.

Purification of co-expressed DmoB136 and DmoA

Frozen, resuspended cells were thawed, mixed with a protease inhibitor tablet (ThermoFisher) and lysozyme (1 mg/mL), and incubated at room temperature for 30 minutes with gently mixing. Cells were lysed using a Q700 sonicator (Qsonica) with a total run time of 10 minutes, 10 second pulse-on and 30 second pulse-off at an amplitude of 40.0 amplitude. Lysed cells were centrifuged at 11,000 rpm, 4 °C, for 1 hour and the supernatant was collected.

The cell soluble lysate was loaded onto a HiTrap Chelating HP column loaded with Nickel (GE Biosciences) at 1 mL/min previously equilibrated with 10 CV of Buffer A (50 mM Tris, 500 mM NaCl, 10% glycerol, pH 8.0). Nonspecific proteins were removed following a 25 CV wash with Buffer A. A linear gradient from 0-100% Buffer B (50 mM Tris, 500 mM NaCl, 10% glycerol, 500 mM imidazole, pH 8.0) spanning 20 CVs was performed and fractions were collected. Fractions were analyzed by SDS-PAGE and/or NADH oxidation activity as described below. Active fractions or fractions containing proteins corresponding to MW of DmoB136 and/or DmoA were pooled, concentrated down via a 10 kDa MWCO membrane (Millipore), and run on a Sephadex G-75 size exclusion column at 0.3 mL/min previously equilibrated with buffer C (50 mM Tris, 150 mM NaCl, 10% glycerol, pH 8.0). Fractions were collected every 3.33 minutes and analyzed as described above.

Protein expression and purity analysis by SDS-PAGE

Proteins fractions from each purification step were analyzed by SDS-PAGE. Samples were prepared by adding SDS reducing buffer (69.45 mM Tris-HCl pH 6.8, 11.1% glycerol, 1.1% SDS, 0.005% bromophenol blue, 2.5% 2-mercaptoethanol) to each fraction. The samples were boiled for 5 minutes before being loaded into an SDS-PAGE gel (15%) along with protein standards. Gels were loaded with Precision Plus Protein™ Dual Color Standards (Bio-Rad) for the protein screening, and PageRuler™ Prestained Protein Ladder, 10 to 180 kDa (ThermoFisher) for expression in C41(DE3). The gels were run at 200 V for 40-60 minutes then stained with Coomassie Blue. SDS-PAGE gels were de-stained using a de-stain solution (40% methanol, 7% glacial acetic acid).

NADH oxidation activity

The oxidation of NADH and reduction of FMN by DmoB136 was monitored using the absorbance at 340 nm and kinetics software using an 8453 UV-Visible Spectrophotometer (Agilent Technologies). Program specifications monitored 340 nm with a single reference background correction at 700 nm. A sample was obtained every second for 120 seconds and the slope of the line calculated by assuming a zero-order reaction. The slope of the line was used in Beer's law in combination with the extinction coefficient of NADH of 6,220 $M^{-1}cm^{-1}$ to calculate the enzyme's activity. Reactions were initiated by the addition of protein to the reaction tube containing; 20 mM PIPES-HCl (pH 7.4), 1 mM NADH, 3 µM FMN, and 5 µM DTT. Protein concentration was calculated using the absorbance at 280 nm and the extinction coefficient for DmoB136 of 3,105 $M^{-1}cm^{-1}$.[22]

Results

Competent cell lines were screened for co-expression, and aliquots were chemically lysed using B-PER Complete Bacterial Protein Extraction Reagent and soluble and insoluble proteins analyzed by SDS-PAGE. Figure 13 shows the crude protein analysis of BL21(DE3) cells grown overnight at 16 °C that were either not induced or induced with 200 µM or 1 mM, and it is a representative gel for each cell line. Lanes 1, 4, and 6 contain the insoluble proteins from non-induced cells, 200 µM IPTG induced cells, and 1 mM IPTG induced cells, respectively. Lanes 3, 5, and 7 contain the soluble proteins from non-induced cells, 200 µM IPTG induced cells, and 1 mM IPTG induced cells, respectively. Lane 2 contains the Bio-Rad Precision Plus Protein™ Dual Color Standards. The proteins of interest, DmoB136 and DmoA, are expected at 16 kDa and 53 kDa, respectively. Though there are noticeable protein bands

around 53 kDa in both the soluble and insoluble fractions no discernable protein overexpression is observed with this method. The protein observed at ~ 15 kDa is due to the lysozyme added during lysis and can be seen in every lane (Figure 13). Though there was indication of protein bands, no discernable conclusions could be made from these results in relation to DmoA and DmoB136 coexpression. Therefore, small-scale affinity chromatography was pursued to visualize expression.

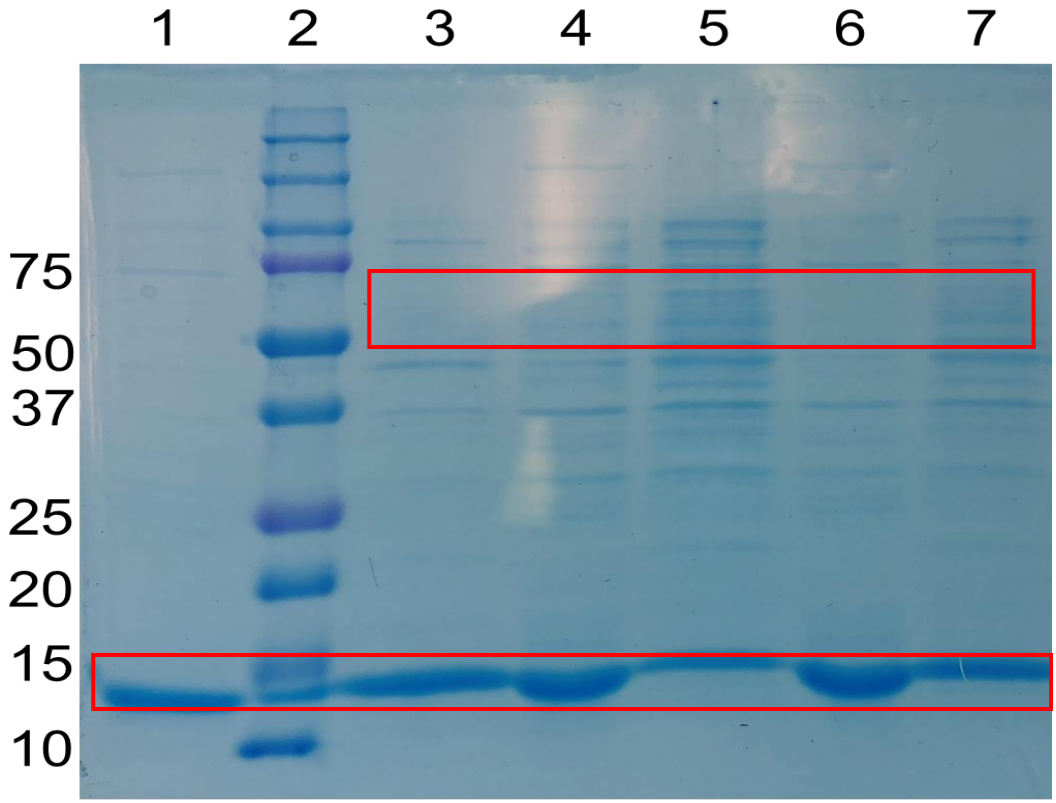

Figure 13. 12.5 % SDS-PAGE gel of protein co-expression in BL21. Lane 2 shows the molecular weight marker (kDa). Lanes 1, 4, and 6 contain the insoluble protein fractions from non-induced cells, 200 µM induced cells, and 1 mM induced cells. Lanes 3, 5, and 7 contain the soluble protein fractions from non-induced cells, 200 µM induced cells, and 1 mM induced cells. Equal volumes of each protein fraction were added to each lane.

Based on crude protein analysis, cell pellets with different growth temperatures and inducer concentrations were chosen for mechanical lysis by sonication, purified by a 0.2 mL

resin bed Ni-affinity column, and analyzed by SDS-PAGE. Figure 14a shows the purification of proteins expressed in BL21(DE3) grown overnight at 16 °C (200 µM IPTG), and lane 2 contains Bio-Rad Precision Plus Protein™ Dual Color Standards. Figure 14b shows the purification of proteins expressed in C41(DE3) grown overnight at 16 °C (500 µM IPTG), the molecular marker is in lane 4. The stepwise imidazole elution can be seen in lanes 4-7 in Figure 14a and in lanes 3-7 in Figure 14b. In Figure 14a, no protein is observed around 53 kDa in any lanes, but in lane 5, two bands can be seen around 16 kDa. In Figure 14b, lanes 3 and 6 both contain protein around 53 kDa as well as 16 kDa.

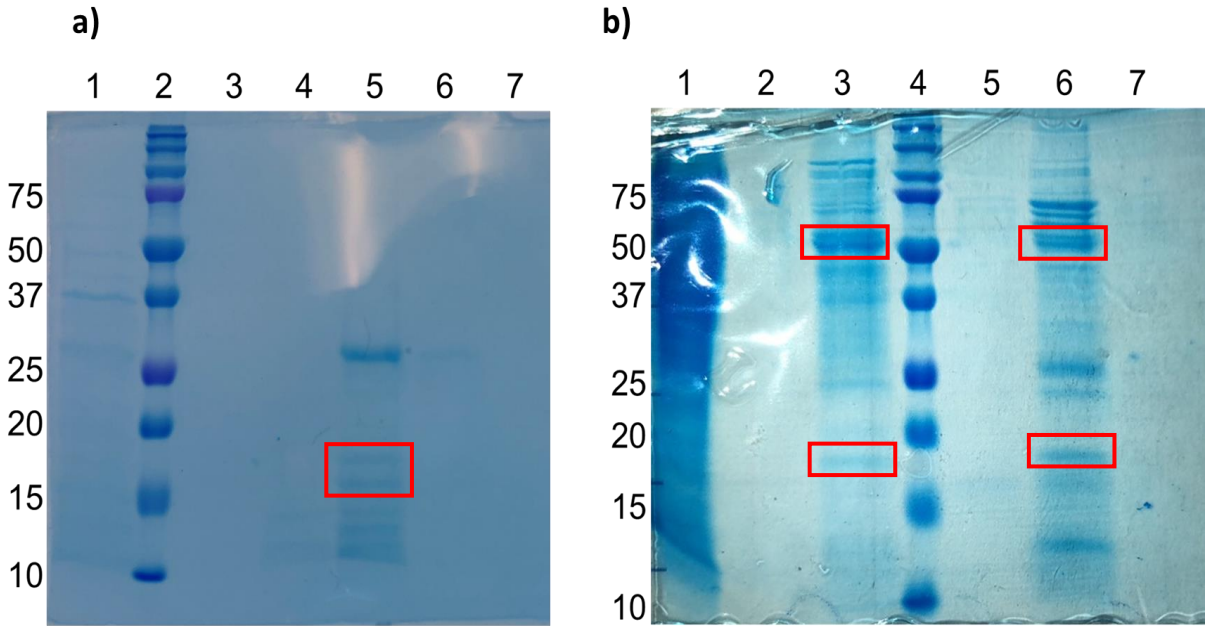

Figure 14. 12.5 % SDS-PAGE gels of DmoB136 and DmoA co-expression purified by HisPur Ni-NTA Spin Column affinity chromatography in BL21(DE3) (a) and C41(DE3) (b). (a) Lane 2 shows the molecular weight marker (kDa). Lanes 1 and 3 show the protein load and wash, respectively. Lanes 4-7 show the step wise imidazole elution. (b) Lane 4 shows the molecular weight marker (kDa). Lanes 1 and 2 show the protein load and wash, respectively. Lanes 3-7 show the step wise imidazole elution. Equal volumes of the protein fraction were added to each lane.

Based on the small-scale affinity chromatography, C41(DE3) *E. coli* cells co-expressing DmoB136-DmoA were upscaled, lysed by sonication, purified by Ni-chelating affinity chromatography, and purified fractions were analyzed by SDS-PAGE (Figure 15). Lanes 2-5 contain the lysate, insoluble protein pellet, protein load, and wash, respectively. Lanes 6-15 correspond to the linear gradient with increasing concentrations of imidazole. Lanes 6, 8, 9, 10, and 11 appear to contain bands around 53 kDa when compared to the PageRuler™ Prestained Protein Ladder. Lanes 4, 6, 9, and 10 appear to contain bands around 16 kDa when compared to the PageRuler™ Prestained Protein Ladder, though faint in comparison to other protein bands (Figure 15). Both lanes 9 and 10 contain bands which correspond to possible co-expression of DmoA and DmoB. These proteins are present in low imidazole fractions consistent with the results in the small-scale purification (Figure 14).

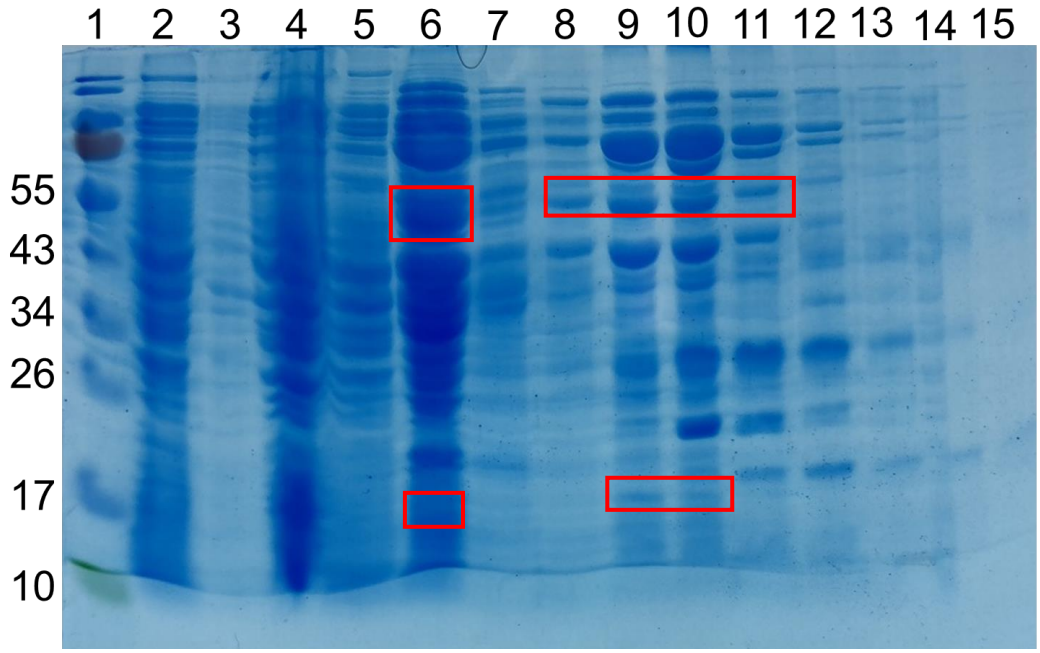

Figure 15. 15 % SDS-PAGE gel of DmoB136 and DmoA co-expression purified by HiTrap nickel-chelating HP affinity chromatography. Lane 1 shows the molecular weight marker (kDa). Lanes 2-5 contain the lysate, pellet, protein load, and wash, respectively. Lanes 6-15 correspond to the linear gradient with increasing concentrations of imidazole. Equal amounts of each protein fraction were added to each lane.

Fractions potentially containing DmoB136 from Figure 15 were analyzed for activity by monitoring the oxidation of NADH by FMN using the absorbance at 340 nm. Since no A_{280} was taken at this stage, no protein concentrations were known. Lane 10 had the highest activity compared to other lanes, and activity decreased by nearly half as the volume of the sample added also decreased by half (Figure 16). Activity from lane 10 was double that of the activity from Lane 11, and no activity was observed when no protein from lane 10 was added (Figure 16).

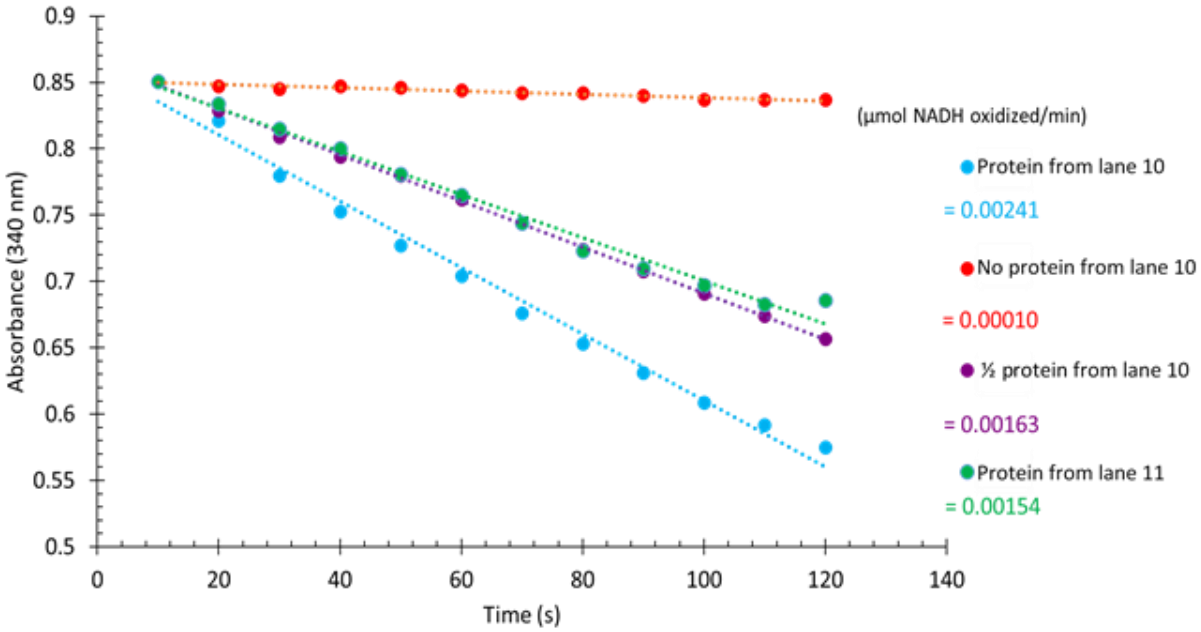

Figure 16. Activity assay measuring oxidation of NADH by FMN of Nickel fractions from C41(DE3). Absorbance at 340 nm over 120 second at different protein volumes from lane 10 compared to proteins in lane 11 from Figure 15.

Active fractions, lane 10 in Figure 15, were concentrated and purified by a Sephadex G75 size-exclusion column and the fractions were analyzed by SDS-PAGE. None of the lanes contain distinct, large bands around 53 kDa when compared to the PageRuler™ Prestained Protein Ladder; however, Lanes 8-12 appear to contain bands around 16 kDa when compared

to the PageRuler™ Prestained Protein Ladder (Figure 17). It should be noted that there is an overall dramatic decrease in total protein compared to that observed in the Nickel Chelating-HP column. There is also a fairly distinct protein band observed at 26 kDa in all of the size exclusion fractions.

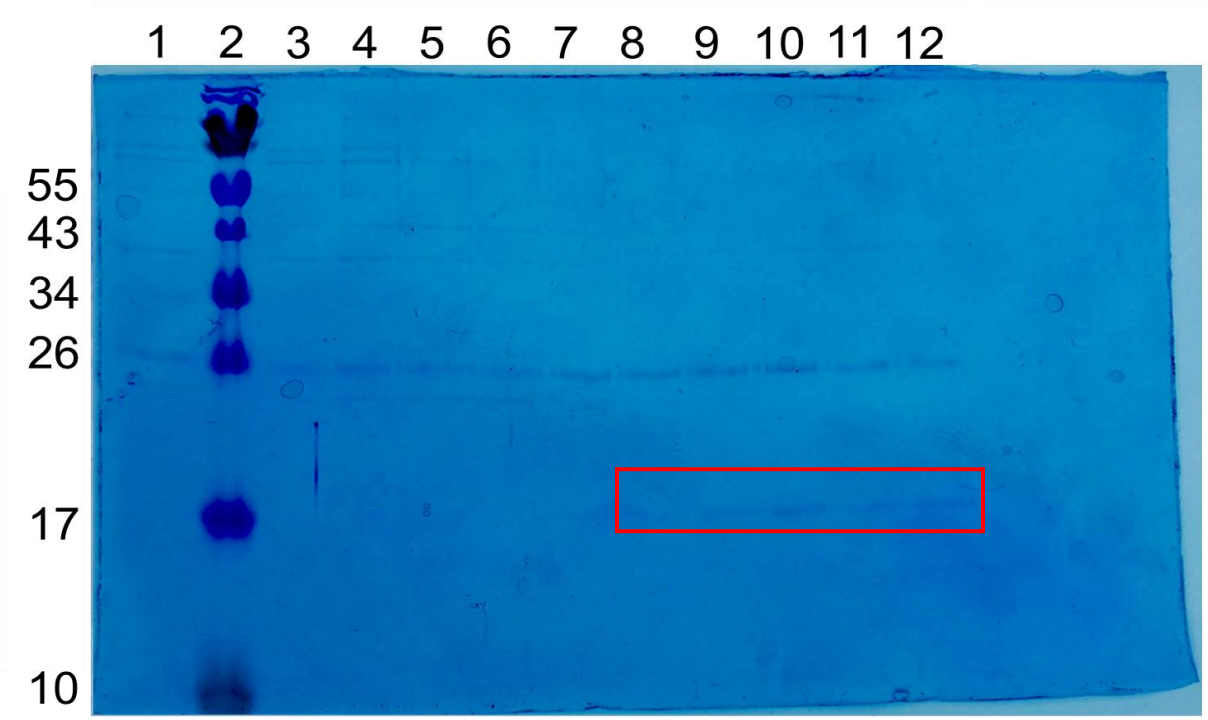

Figure 17. SDS-PAGE gel of coexpressed DmoB136-DmoA purified by Sephadex G75 size exclusion chromatography. Lane B shows the molecular mass markers (kDa). Equal amounts of each protein fraction were added to each lane.

Specific activity was measured after Ni-chelating affinity chromatography and after Sephadex G75 size-exclusion chromatography with and without FMN. The specific activity in the presence of FMN was 0.257 µmol NADH oxidized/min/mg protein after background correction with a control run without FMN from the Ni Chelating HP column (Table IV). The specific activity from the Sephadex G75 size-exclusion chromatography fractions was 0.938

μmol NADH oxidized/min/mg protein in the presence of FMN after background correction with a no FMN control run (Table IV).

Table IV. Specific activity of DmoB136 with and without FMN after purification

Column	Specific Activity with FMN (μmol NADH oxidized/min/mg protein)	Specific Activity without FMN (μmol NADH oxidized/min/mg protein)
Ni-chelating HP	0.257	0.0185
Sephadex G75	0.938	0.0154

Discussion

The gel for crude protein analysis in BL21(DE3) is representative for each screened cell line (Figure 13). Faint protein bands can be seen in every lane, though no clear overexpression is observed using the B-PER lysis method. It was expected that the overexpressed recombinant proteins would be found in lanes 3, 5, and 7 in the soluble fractions. The bands around 53 kDa were found in both soluble and insoluble fractions, providing indeterminate results in relation to DmoA protein expression. The bands around 16 kDa were either not observed or hard to distinguish since the lysozyme present in each sample is roughly 15 kDa. Overall, initial results from crude protein analysis by SDS-PAGE proved inconclusive, and small-scale affinity chromatography was employed to try and resolve bands and provide conclusive results.

The gels from Figure 14 compare the protein co-expression after Ni-NTA affinity chromatography in BL21(DE3) and C41(DE3) both grown overnight at 16 °C and induced with 200 μM IPTG and 500 μM, respectively. In Figure 14a, no band around 53 kDa is observed in any fraction, meaning that DmoA was potentially not expressed or expressed in such low yields it is not observable by SDS-PAGE; however, two bands can be seen around 16 kDa in lane 5. The results from this column do not demonstrate the co-expression of DmoB136 and

DmoA in BL21 cells. There are bands indicative of co-expression seen in the C41(DE3) cell line, however. In both lanes 3 and 6 protein around 53 kDa and 16 kDa can be observed, with near stoichiometric amounts in lane 6. Based on the comparison of protein analysis by SDS-PAGE from the Ni-NTA Spin Columns, C41(DE3) were chosen for optimal co-expression.

Sizes of protein from the gels containing protein purified by Ni-chelating affinity chromatography can be determined through comparison of bands to the PageRuler™ Prestained Protein Ladder. Proteins around 16 kDa and 53 kDa were expressed in low imidazole fractions, which are close in molecular weight to DmoB136 and DmoA respectively. These results indicate a possible interaction between subunits following His-tag purification which is consistent with the results in the small-scale purification. It is likely that the two subunits co-expressed, though sequence identification by Mass Spectrometry is necessary to confirm this result. This result is surprising given the elution in the low imidazole fractions indicating that the DmoB136 has weak interaction with the Nickel. It was expected that both proteins or at minimum DmoB136 would elute in the high concentration imidazole fractions.

Following affinity chromatography, NADH oxidation activity of DmoB136 was performed on various fractions. This assay is used as the first measurement due to its sensitivity and ease compared to the assay to measure DmoA activity. The protein activity from fraction 10 was the highest relative to the other fractions tested, indicating DmoB136 expression. When equal concentration of protein from fraction 11 was added to the reaction mixture, the activity observed was nearly half of the activity observed from fraction 10. When half the concentration of protein from fraction 10 was added to the reaction mixture, the activity decreased proportionally, suggesting an enzyme dependent reaction. After

determining concentrations of protein by A_{280}, the specific activity was higher in the presence of FMN than in the absence of FMN. These results indicate successful expression of DmoB136 as NADH oxidation is occurring as a result of enzyme and the FMN cofactor. No assays were run in the presence of the DMS substrate to observe faster rate couplings with both subunits present. In addition, direct product detection from DmoA activity is also necessary to determine whether co-expression is occurring or just expression of the reductase DmoB136 subunit.

It can be determined from the gels containing protein purified by Sephadex G75 size-exclusion chromatography that there was an overall decrease in protein yield; however, purification was successful as there was an extreme decrease in contaminant proteins despite the loss of protein. Two predominate protein bands are found on the gel at 26 kDa and 16 kDa. Fractions throughout the purification were tested for NADH oxidation as above, and the 16 kDa protein fractions from lanes 8-12 were active compared to the remaining fractions. The specific activity in the presence of FMN was nearly 4 times than after Ni-affinity chromatography which is to be expected after successful purification, as the amount of protein should decrease as undesired proteins are filtered out. Dividing the activity by this reduced amount of protein yields a higher specific activity. The activity without FMN was low and roughly the same as that after affinity chromatography. This NADH specific activity in combination with the purified protein band at ~16 kDa supports the finding that the expression of DmoB136 was successful. The absence of a predominate protein band ~ 53 kDa could be a result of a decrease in the salt concentration in each equilibration buffer for each purification strategy, disrupting potential ion-ion interactions between subunits. This will

need to be tested further using higher salt concentrations in future gel filtrations. These results could indicate that the tight association between the two subunits demonstrated by Boden et al.[11] is not observed in this recombinant co-expression study.

Chapter IV: Conclusion and Future Directions

Conclusion

Overall, these results suggest the successful expression and purification of the DmoB136 subunit alone. They also suggest the DmoA subunit was also expressed but did not purify alongside DmoB136 in a tight association under the gel filtration conditions tested, possibly due to the loss of electrostatic interactions. Based on previous studies conducted by members of the Culpepper lab where the recombinant expression of the individual subunit DmoB136 lead to the formation of inclusion bodies, so it is plausible that DmoA was also expressed since its presence has been shown to aid in the expression of DmoB136. A tight association between the subunits was observed by Boden et al. in DMS monooxygenase expressed natively in *H. sulfonivorans*,[9] it was expected that fractions containing DmoB136 would consequently contain DmoA at stoichiometric levels. The gels did not indicate stoichiometric amounts of DmoB136 and DmoA, though the yields are low and may not be detecting both proteins. Enzyme activity on DmoB136 shows NADH oxidation in the presence of FMN, though testing activity in the presence of the substrate DMS is necessary to confirm whether the DmoA subunit is associating with the DmoB136 subunit.

Although much has been learned, there are still experiments that could strengthen the results from this co-expression study. A native-PAGE or MALDI-TOF mass spectrometry could be performed in order to determine the native quaternary structure of the co-expressed proteins. A Western blot could be performed on the crude protein since DmoB136 contains a His_6-tag and DmoA contains an S-tag. The detection limits of this technique are lower and the specificity for our proteins higher in comparison to SDS-PAGE. The results from

a Western blot would confirm the expression of both subunits, and when coupled with activity results, it would further help in the selection of fractions for purification. These results show that further protein analysis and purification strategies are necessary to purify DmoA from this co-expression since DmoA was not observed in later purification fractions with DmoB136. Once DmoA has been successfully isolated, activity trials monitoring product formation can be performed in the presence and absence of DmoB136 in order to further characterize the interaction between subunits. Finally, Michaelis-Menten kinetics could determine the substrate affinity for each subunit.

The focus of this project was to engineer a single vector (pCDFDUET-1) containing the genes of both *dmoB136* and *dmoA,* optimize growth for protein co-expression, and analyze enzyme kinetics and activity in DMS degradation. It was hypothesized that expressing both subunits simultaneously would allow for the successful expression of DmoB136, and that through co-expression, a tight association between DmoA and DmoB136 would be observed similar to the native protein. The data from this experiment demonstrates that co-expression enabled DmoB136 to be expressed; however, the tight association between subunits is likely not observed, suggesting that DmoB136 may not represent the native binding partner but the expression is aided by the presence of DmoA. It is plausible that the *dmoB176* gene on the *dmo* operon is the native binding partner to DmoA and the same co-expression studies described herein will need to be repeated with this gene candidate in order to determine if a strong subunit:subunit interaction can occur in vitro similar to what is reported in the in vivo studies of DMS monooxygenase from *H. sulfonivorans*.

References

1. Lappalainen H.K.; Kerminen V.; et al.; Pan-Eurasian Experiment (PEEX): towards a holistic understanding of the feedbacks and interactions in the land–atmosphere–ocean–society continuum in the northern Eurasian region; *Atmos. Chem. Phys*.; **2016**; 16: 14421-61.

2. Bentley, R.; Chasteen, T.G.; Environmental VOSCs—formation and degradation of dimethyl sulfide, methanethiol and related materials; *Chemosphere*; **2004**; 55(3): 291-317.

3. Han, Q.; Rossow, W.B.; Chou, J.; Welch, R.M.; Global Survey of the Relationships of Cloud Albedo and Liquid Water Path with Droplet Size Using ISCCP; *J. Climate*; **1998**; 11: 1516–1528.

4. Charlson, R.J.; Lovelock, J.E.; Andreae, M.O.; Warren, S.G.; Oceanic phytoplankton, atmospheric sulphur, cloud albedo and climate; *Nature*.; **1987**; 326(6114): 655–661

5. Yoon, S.H.; Chai, X.S.; Zhu, J.Y.; Li, J.; Malcolm, E.W.; In-Digester Reduction of Organic Sulfur Compounds in Kraft Pulping; *Adv. Environ. Res.*; **2001**; 5(1):91-98.

6. Omura, K.; Swern, D.; Oxidation of alcohols by "activated" dimethyl sulfoxide. A preparative, steric and mechanistic study; *Tetrahedron*.; **1978**; 34(11): 1651–1660

7. Glindemann, D.; Novak, J.; Witherspoon, J.; Dimethyl Sulfoxide (DMSO) Waste Residues and Municipal Waste Water Odor by Dimethyl Sulfide (DMS): the North-East WPCP Plant of Philadelphia; *Environ. Sci. Technol*; **2006**; 40(1): 202–207.

8. Lomans B.P.; van der Drift, C.; Pol, A.; Op den camp, H.J.M.; Microbial cycling of volatile organic sulfur compounds in anoxic environments; *Wat. Sci. Tech.*; **2002**; 45(10): 55-60.

9. Smith, N.A.; Kelly, D.P.; Isolation and Physiological Characterization of Autotrophic Sulphur Bacteria Oxidizing Dimethyl Disulphide as Sole Source of Energy; *J. Gen. Microbiol.*; **1988**; 134: 1407-17.

10. Schafer, H.; Isolation of Methylophaga spp. from Marine Dimethylsulfide-Degrading Enrichment Cultures and Identification of Polypeptides Induced during Growth on Dimethylsulfide; *Appl. Environ. Microbiol.*; **2007**; 73(8): 2580-91.

11. Boden, R.; Borodina, E.; Wood, A.; Kelly, D.; Murrell, C.; Schafer, H.; Purification and Characterization of Dimethylsulfide Monooxygenase from *Hyphomicrobium sulfonivorans*; *J. Bacteriol*.; **2011**; 193(5): 1250-58. doi:10.1128/JB.00977-10.

12. Ellis, R.; The FMN-dependent two-component monooxygenase systems; *Arch. Biochem. Biophys.*; **2010**; 297: 1-12.

13. Huijebrs, M.M.E.; Montersino, S.; Westphal, A.H.; Tischler, D.; van Berkel, W.J.H.; Flavin dependent monooxygenases; *Arch. Biochem. Biophys.*; **2014**; 544: 2-17.

14. Scheich, C.; Kummel, D.; Soumailakakis, D.; Heinemann, U.; Bussow, K.; Vectors for co-expression of an unrestricted number of proteins; *Nucleic Acids Res.*; **2007**; 35(6): e43.

15. Lee, J.K.; Zhao, H.; Identification and Characterization of the Flavin: NADH Reductase (PrnF) Involved in a Novel Two-Component Arylamine Oxygenase; *J. Bacteriol.*; **2007**; 189(23): 8556-63.

16. Chen, Y.H.; Wang, C.C.; Greenwell, L.; Rix, U.; Hoffmeister, D.; Vining, L.C.; Rohr, J.; Yang, K.Q.; Functional Analyses of Oxygenases in Jadomycin Biosynthesis and Identification of JadH as a Bifunctional Oxygenase/Dehydrase; *J. Biol. Chem.*; **2005**; 280(23): 22508-14.

17. Blake, J.A.R.; Pritchard, M.; Ding, S.; Smith, G.C.M.; Burchell, B.; Wolf, C.R.; Friedberg, T.; Coexpression of a human P450 (CYP3A4) and P450 reductase generates a highly functional monooxygenase system in *Escherichia coli*; *FEBS Lett.*; **1996**; 397: 210-4.

18. Corpet, F.; Multiple sequence alignment with hierarchical clustering; *Nucl. Acids Res.*; **1988**; 16(22): 10881-90.

19. Papaneophytou, C.P.; Kontopidis, G.; Statistical approaches to maximize recombinant protein expression in *Escherichia coli*: A general review; *Protein Expr. Purif.*; **2014**; 94: 22-32.

20. Novagen; Competent Cells; *EMD Biosciences inc.*; **2004**; User Protocol TB009 Rev. F 0104.

21. Lucigen; OverExpress® Chemically Competent cells; *Lucigen Corporation*; **2018**; MA031.

22. Dawson, R.B.; *Data for biochemical research*; 3rd ed. Oxford: Clarendon Press; **1985**; p. 122.